Real-time control of a robot arm using simultaneously recorded neurons in the motor cortex

John K. Chapin[1], Karen A. Moxon[1], Ronald S. Markowitz[1] and Miguel A. L. Nicolelis[2]

[1] *Department of Neurobiology and Anatomy, MCP Hahnemann School of Medicine, Philadelphia, Pennsylvania 19129, USA*

[2] *Department of Neurobiology, Duke University Medical Center, Durham, North Carolina 27710, USA*

Correspondence should be addressed to J.K.C. (chapinj@mcphu.edu)

To determine whether simultaneously recorded motor cortex neurons can be used for real-time device control, rats were trained to position a robot arm to obtain water by pressing a lever. Mathematical transformations, including neural networks, converted multineuron signals into 'neuronal population functions' that accurately predicted lever trajectory. Next, these functions were electronically converted into real-time signals for robot arm control. After switching to this 'neurorobotic' mode, 4 of 6 animals (those with >25 task-related neurons) routinely used these brain-derived signals to position the robot arm and obtain water. With continued training in neurorobotic mode, the animals' lever movement diminished or stopped. These results suggest a possible means for movement restoration in paralysis patients.

Pioneering studies suggested that motor information in the cortex is coded through the combined actions of large populations of widely tuned neurons rather than by small numbers of highly tuned neurons[1]. Several systems provide further evidence for this 'distributed coding' in brain function[2,3]. However, such investigations used serial recordings of single neurons averaged over repeated trials, and therefore could not demonstrate neuronal population encoding of brain information on a single-trial basis. Techniques for simultaneous (parallel) neuronal population recording enables surprisingly rich encoding of information in the brain using randomly sampled neuronal populations, especially in the somatosensory[4–6] and limbic systems[7].

We addressed these issues by simultaneously recording from arrays of electrodes chronically implanted in the primary motor (MI) cortex and ventrolateral (VL) thalamus in rats trained in a forelimb movement task. We asked three questions. First, how well can linear or nonlinear mathematical transformations of neuronal population activity in the MI cortex and/or VL thalamus encode forelimb movement trajectories? Second, can these 'motor codes' be used to generate an online 'neuronal population function' to control a robotic arm in real time with sufficient accuracy to substitute for animal forelimb movement in the trained motor task? Third, might training in this neurorobotic mode (rewarding the neural activity itself) change or extinguish the previously conditioned movement?

Results

Rats were first trained to obtain a water reward by depressing a spring-loaded lever to proportionally move a robot arm to a water dropper (Fig. 1.). On release, water was transferred to the mouth passively. Neuronal population recordings in this behavioral mode ('lever-movement/robot-arm') were used to derive neuronal population functions that predicted forelimb movement. A multichannel electronic device then calculated, in real time, the inner product of this neuronal population function (a 32-element weight matrix) times integrated spiking activity of 32 simultaneously recorded neurons. The output was a single analog voltage signal used to position the robot arm. Robot arm control could be arbitrarily switched from the lever (actual forelimb movement) to this brain-derived neuronal population signal.

Six rats were trained to control the robot arm by moving a lever and were then surgically implanted with recording electrode arrays (see Methods). After recovery, populations of 21–46 (mean, 33.2) single neurons were discriminated from these electrodes during lever movement to control a robot arm; from rat 1, we simultaneously recorded 46 neurons (32 in MI and 14 in VL; Fig. 2). The plot depicts averaged responses centered around onset of forelimb extension of each neuron and of all MI or VL cells over 44 trials. All but 5 neurons modulated firing over this task (≥ 99% confidence level; Kolmogorov-Smirnov). In 6 MI-implanted animals, 16–41 neurons (mean, 33.5) showed significant task correlation.

Movement trials began from rest when the animal reached for the lever using antebrachial (forearm) flexion followed by brachial (arm) flexion and finally carpal (paw) extension. Just above the lever, the forepaw flexed rapidly downward with antebrachial extension, touching the lever within a mean of 41 ms. Continued extension pressed the lever to position the robot arm toward a water drop. The antebrachium was then flexed to release the lever, allowing the arm to return to the rat.

Analysis of repeated trials (using EMG and videos) revealed a consistent sequence of forelimb movements. Peri-event histograms and rank-ordered raster plots were used to characterize each neuron's primary motor correlate in terms of forelimb movement elements during these trials. Rank-ordered rasters were particularly effective in resolving the part of the observed movement sequence best correlated with neuronal activity. Four general categories of task-related neurons were observed (Fig. 3).

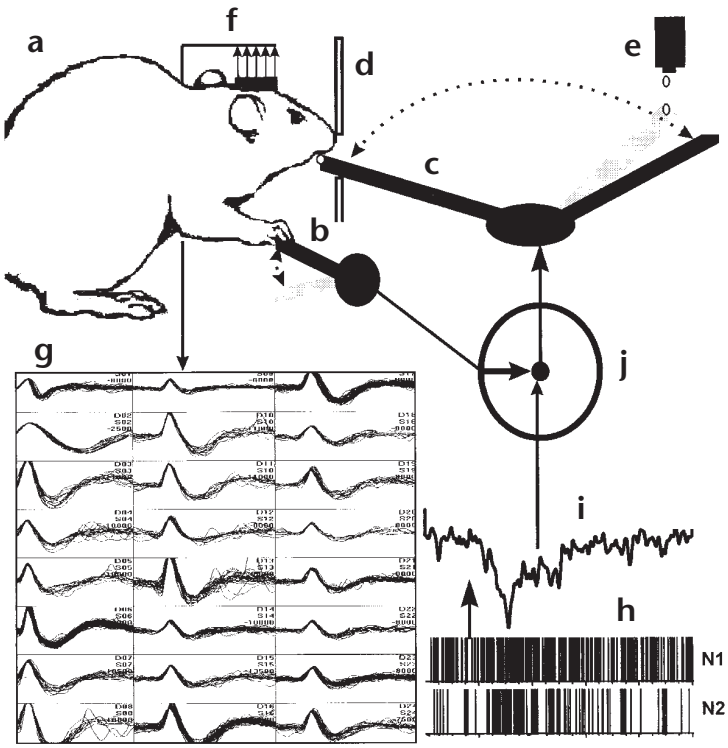

Fig. 1. Experimental protocol. **(a)** 'Lever-movement/robot-arm' mode: rats were trained to press a lever **(b)** for a water reward; displacement was electronically translated to proportionally move a robot arm **(c)** from rest position through a slot in barrier **(d)** to a water dropper **(e)**. The robot arm/water drop moved passively to the rest position (to the rat). **(f)** 'Neuronal-population-function/robot-arm' mode: Rats were chronically implanted with multi-electrode recording arrays in the MI cortex and VL thalamus, yielding simultaneous recordings of up to 46 discriminated single neurons. **(g)** Superimposed waveforms of 24 such neurons. **(h)** Sample spike trains of two neurons (N1, N2) over 2.0 s. **(i)** Neuronal-population (NP) function extracting the first principal component of a 32-neuron population. **(j)** Switch to determine input source (lever movement or NP function) for controlling robot-arm position. In experiments, rats typically began moving the lever. The input was then switched to the NP function, allowing the animal to obtain water through direct neural control of the robot arm.

'Pre-flexion' neurons (13% of task related in MI; 43% in VL) discharged before brachial flexion to initiate lever reach; 'flexion' neurons (16% in MI; 21% in VL) discharged mainly after the onset of antebrachial flexion; 'pre-extension' neurons (28% in MI; 15% in VL) were best correlated with the pre-onset and onset of carpal flexion initiating antebrachial extension before forepaw placement on the lever, and 'extension' neurons (43% in MI; 21% in VL) were correlated somewhat with antebrachial extension onset and strongly with placement of the forepaw on the lever. This last category corresponded closely with previously described 'forepaw placing' neurons in rat sensorimotor cortex[8]. Both pre-extension and extension neurons began to discharge ~30–50 ms before forepaw contact. Most of these discharged more strongly before touch than during movements without contact. Moreover, the timing of these pretouch neural response peaks corresponded to timing of sensory gating in neurons in SI cortex[9–12]. These neurons also exhibited 'motor' activity comparable to the premovement discharges described in the MI cortices of many species[13–15] (Fig. 3b). The peri-event histograms centering around triceps EMG onset in trials in which the forepaw was momentarily held motionless on the lever before pressing demonstrate that the combined activity of the pre-extension and extension neurons preceded detectable lever movement by as much as 150 ms, and triceps muscle EMG by 100 ms.

Average amplitude of ensemble activity peaked in the period before paw contact with the lever (Fig. 2). These peaks represented maximal discharge of the majority of sampled neurons (74% in Fig. 2; 71% across all 6 animals) and were therefore present in neuronal population (NP) ensemble averages. By selecting neurons by peak pre-lever-movement amplitude, it was possible to create neuronal population functions composed exclusively of neurons (16–32) expressing this tuning function (Figs. 5 and 6).

Neuronal population coding in spatiotemporal domain

Because of the heterogeneity of firing characteristics in these neuronal ensembles, distinct cross-neuron discharge patterns were associated with each phase of forelimb movement. Indeed, multivariate analysis of variance (MANOVA) yielded significant differences between multineuron discharge patterns measured across the four movements in Fig. 2 ($F_{141,2828} = 12.3$, $p < 10^{-9}$ for this case, and $p < 10^{-6}$ for the other animals). Thus conventional statistical approaches such as discriminant function analysis (DFA)[6–7,21] could be used to mathematically transform population data into 'neuronal population functions' that predicted each movement on a per-trial basis (82% overall accuracy). Though DFA-defined linear neuronal-population functions generally predicted movement direction (flexion versus extension), they were less able to predict exact timing or displacement. This resulted from the neurons' tendency to phasically discharge before onset of movements best associated with their activity, suggesting that temporal in addition to spatial mathematical transformations in the domains may better predict movement from neural activity preceding the movement.

A two- stage process was developed. First, principal components analysis (PCA) was used to decompose the multineuronal covariance in the NP into a small number of uncorrelated components[5,16,17]. As all neurons showed activity before lever movement, the first principal component depicted peaks of NP activity preceding lever movement more accurately than the NP ensemble average in all animals. Simple thresholding (T) of this NP function predicted all lever movements in this experiment, and 87% of lever movements in all animals (Fig. 4b).

Next, artificial neural networks (ANNs) using dynamic back-propagation learning to store temporal information in recurrent connections accurately predicted the lever movement (Fig. 4d, $r = 0.86$) by temporally transforming such NP information. Limiting input to this ANN to the first principal component was sufficient; the second and third components did not improve prediction as measured by the mean-squared error loss function. Analysis of 44 transformations suggested that the ANN used distinct temporal features of the NP signal to predict lever-movement timing and magnitude. Lever movement was predicted by a steeply sloping pre-lever-movement peak (3 in Fig. 4b). The remarkably selective ANN also did not respond to activity patterns lacking the distinctive shape of this peak (for example, at 1 and 2 in Fig. 4b). Similarly, termination of lever movement was correctly predicted within a mean 64 ms by a

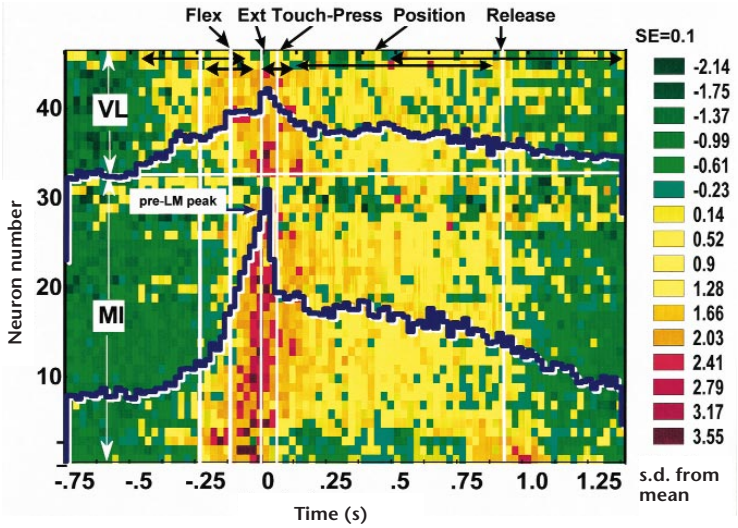

Fig. 2. Color-coded peri-event population response plot shows activity of 46 simultaneously recorded neurons in the MI cortex and VL thalamus of rat 1, averaged around the onsets of 44 pressing movements. Individual neurons (MI, 32; VL, 14) are numbered on the *y*-axis. Time (*x*-axis) is measured from lever movement. Colors depict instantaneous neuronal firing rates (25-ms bins), standardized for each neurons' peri-event histogram by subtracting the mean and dividing by the standard deviation (s.d.). White, vertical lines indicate mean and black horizontal arrows the ranges of movement onset. Average times of onset of flexion ('Flex'), extension ('Extens'), 'Touch-press', 'Position' and 'Release' are indicated by labels above the plot. The blue lines across the MI and VL population-response plots represent ensemble averages of the population activity in these regions over 44 trials. The 'pre-LM peak' immediately precedes onset of lever movement.

distinctively sharp drop in NP activity (4 in Fig. 4b). Similar NP properties were found in the other five animals in which MI/VL forelimb neurons were recorded.

Further analysis of such ANNs suggested that they 'learned' to make such predictions by encoding distinct temporal response functions into their recurrent circuitry. For example, one trained ANN responded to a single test impulse that peaked with 300-ms latency and subsequently decayed over 1s (inset above Fig. 4d). This output timing was remarkably similar to the temporal correlation between the pre-lever-movement peak and the lever movement (Fig. 5b). Overall, these findings suggest that movement-related information may be more completely specified by spatiotemporal functions than by purely spatial functions.

Pre-lever-movement peak encodes lever movement

The strength and specificity of this tight relationship between pre-lever-movement NP activity peaks and lever movements was further demonstrated in rank-ordered raster plots and correlation analyses (Fig. 5). In trials in which the pre-lever-movement peak was small (Fig. 5a, top), the initial pressing movement was insufficient, requiring additional lever pressure to obtain water. Lever movement was sufficient to position the robot arm under the water dropper within 500 ms only in trials in which the pre-lever-movement peak was large (Fig. 5a, bottom).

Time-shifted cross-correlation analysis of the same data (Fig. 5b) showed that the NP predicted lever displacement over the 200–500 ms following onset of lever movement (correlation peak labeled 1; $r_{max} = 0.76$; $p < 0.001$). By comparison, NP activity following lever movement was negatively or not correlated with lever movement (2). Moreover, the trough at 3 and peak at 4 both indicate prediction of NP activity by previous movement. This reversal from a prospective ('motor') to a retrospective ('sensory') mode was associated with the transition from pressing to release of the lever, when the animal allowed the spring-loaded lever to push the forelimb upward.

Similar temporal correlations were also found in NPs containing only MI cortical neurons ($r_{max} = 0.79$; $r_{max} = 0.65$ across the 6 animals) and significantly though more weakly, in NP activity of VL thalamic neurons (mean $r_{max} = 0.44$, $p < 0.001$). Finally, these peaks before lever movement were correlated with extensor (triceps) muscle EMG activity (mean $r_{max} = 0.64$ in 2 animals), beginning a mean 26 ms before onset of lever movement and continuing for 100–400 ms. As the lever was spring loaded, the NP activity in MI and VL preceding lever movement was correlated both with the force[13,18–20] and the tra-

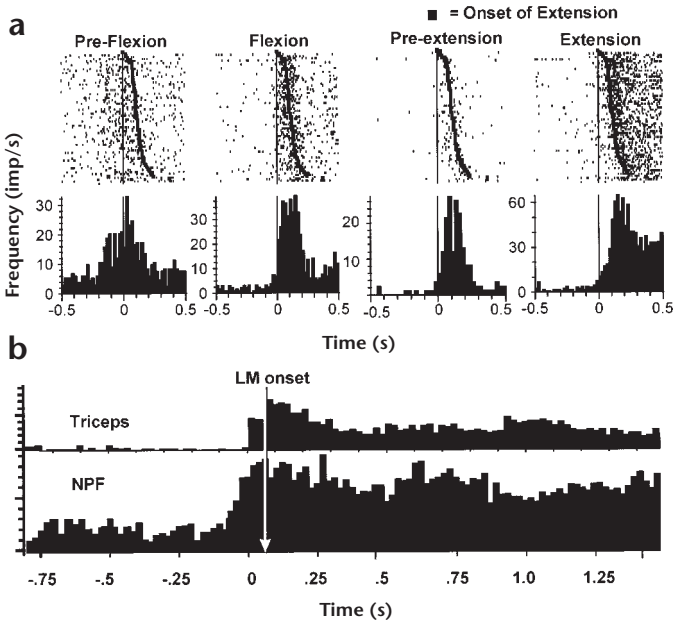

Fig. 3. Categories of recorded neurons. **(a)** Rank-ordered peri-event rasters and histograms centered around onset of antebrachial flexion demonstrate motor correlates of four neuron types. 'Pre-flexion' neurons discharged before flexion through antebrachial flexion, abruptly terminating on carpal flexion and antebrachial extension. 'Flexion' neurons discharged from antebrachial flexion through antebrachial extension. 'Pre-extension' neurons discharged phasically up to 50 ms before carpal flexion. 'Extension' neurons discharged phasically and then tonically during antebrachial extension in reach-to-touch movements. Vertical scales show instantaneous average firing rate. **(b)** Premovement neural activity during 10 trials (in rat 3); rat started lever-press with paw on bar but did not reach. Trials are averaged around the onset of triceps EMG activity. 'Triceps', muscle EMG; 'NPF', NP activity of 28 MI cortical neurons over the same 10 trials. Mean NP activity led EMG onset by 63 ms; bar movement (white arrow) lagged by 33–66 ms.

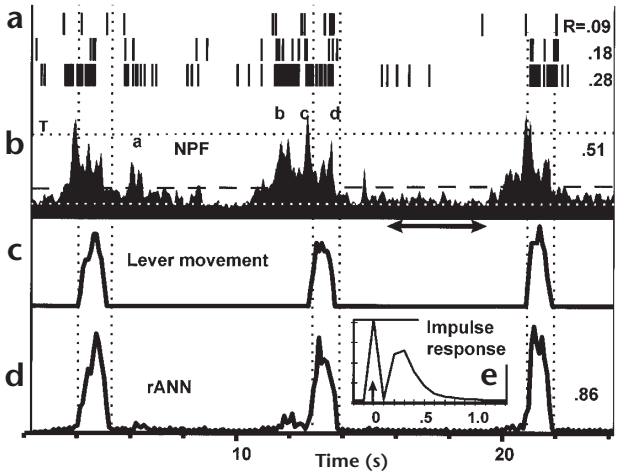

Fig. 4. Comparison of modes of movement 'coding' in lever-movement/robot-arm mode. Vertical dotted lines indicate starts and stops of lever movement. **(a)** Spike train rasters from three neurons showing low, middle and high correlation with forelimb movement. **(b)** Stripchart of 32-neuron NP function (NPF) binned at 20 ms and smoothed over 2-bin windows. Activity peaks relating to overall magnitude of limb movement are shown at 1, 2, 3 and 4. White, dotted lines mark mean activity during the resting period (two-headed arrow). Black, dashed lines mark 3 s.d. above mean activity. **(c)** Vertical position of the lever; threshold 'drinking' position is at bottom and 'water drop' position at top. **(d)** Transformation of NPF **(b)** with a recurrent neural network (rANN) to predict lever movement timing and magnitude as in **(c)**. **(e)** 'Impulse response' shows the response of this ANN to an input pulse (arrow) equivalent to one spike; impulse-response amplitude is about 1% maximum in **(d)**. For both **(d)** and **(e)**, bin width is 100 ms. Horizontal axes are the same for **(a–d)**. Coefficients of correlation (*r*) with lever position in **(c)** are shown at right for spike trains and NP functions.

jectory (timing and magnitude) of lever movement. Moreover, NP activity preceding lever movement was slightly better correlated with lever displacement than velocity of lever movement (measured over 100 ms time bins). The same NP activity preceding lever movement and, after conversion to instantaneous velocities, lever displacement in Fig. 5b were used to obtain a time-shifted correlogram (Fig. 5c). By comparison with Fig. 5b (where $r_{max} = 0.76$), the maximum correlation between the activity peak preceding and velocity after lever movement is highly significant, but slightly smaller (1 in Fig. 5c; $r_{max} = 0.51$; $p < 0.001$), and is limited to the 200 ms following onset of lever movement. Similar results were found in the other animals, yielding a mean $r_{max} = 0.47$ for velocity versus 0.65 for displacement. These findings may also suggest that movement velocity measured 200–500 ms after onset was more significantly correlated than that measured in the 0–100 ms immediately following movement onset with the activity peak before lever movement. This suggests a complex relationship between the peak amplitude preceding lever movement and the final position targeted by training.

Neurorobotic control

Our ultimate aim was to determine whether the animal could use its brain activity, electronically transformed in real-time from on-line NP recordings, to control the robot arm with sufficient accuracy to obtain water. Because the above analyses demonstrated that the NP-function peak amplitude preceding lever movement was proportional to lever movement used to position the robot arm, we hypothesized that NP activity itself could be used to achieve the same positioning. On the other hand, it was not known whether this brief, premovement NP function could substitute for the relatively long-duration limb movement with which it was normally associated.

For this purpose, NP functions were generated (using PCA as above) for neurons selected for strong activity preceding lever movement. To manifest these NPs in real time, a summing amplifier-integrator circuit allowed each of 32 discriminated spike-train input channels to be individually weighted and integrated into a single analog voltage output. Control of the robot arm could be suddenly switched from the lever-movement/robot-arm mode to an NP-function/robot-arm mode (Fig. 1), allowing substitution of the NP function for lever movement as the operant behavior necessary to obtain the water reward. To maintain the normal association between movement of the lever and of the robot arm, animals worked in the lever-movement/robot-arm mode for about five minutes preceding each experimental session. This ensured that the animal continued to initiate conditioned lever movements when the mode was suddenly switched to the NP-function/robot-arm mode. These movements provided direct timing of the animal's motor-behavioral 'intention' as defined by the conditioning task.

Figure 6b shows typical activity of the NP function over 100 seconds following this rat's first switch to NP-function/robot-arm mode. In eight of nine lever movements during this period, the real-time NP function output successfully moved the robot arm to the water-drop position to obtain the water reward (indicated by asterisks). Over the entire 280-second experiment, the animal was 100% efficient (15 of 15 trials) in using NP-function activity to retrieve the water reward when appropriately large-amplitude lever movements were made. In contrast, the NP-function failed to reach threshold and the rat did not receive water in 8 of 11 trials in which lever movements were incomplete (for example, F in Fig. 6b). Two of six animals showed 100% efficiency during complete lever movements; another 2 showed 76% and 91% efficiency on the first try, all of which were sufficient to maintain operant behavior. In the remaining two animals, NP-function signals were only 67% and 54% efficient in generating rewards, insufficient to maintain the behavior for more than 1–2 minutes.

The success of the NP function in maintaining conditioned behavior depended on the strength of activity preceding lever movement relative to its background variability[21]. This was most importantly related to the number and selectivity of the neurons whose activity was integrated to generate the NP function. In Fig. 6b, for example, the NP-function threshold for moving the robot arm to the water dropper was 10.25 s.d. above the mean, but among the 32 neurons used to encode it, mean peak activity preceding lever movement was on average 3.2 s.d. above the mean. Thus, the NP function resolved lever movement much more clearly than any single constituent neuron. Across the 4 successful animals, the activity peaks preceding lever movement were on average 9.2 s.d. above the mean (range, 7.64–10.25), but only 3.6 for the individual neurons. In the 2 unsuccessful rats, the yield of task-related neurons was relatively low (16 and 19), giving relatively weaker activity peaks preceding lever movement (5.2 and 5.7 s.d. above the mean). Thus, an activity peak of 6–8 s.d. above the mean and an NP of 20–25 task-related neurons were required to successfully control the robot arm and maintain conditioning.

These results showed that animals could substitute the NP function for limb movement despite its tendency to lead lever movement, triggering delivery of water before movement onset.

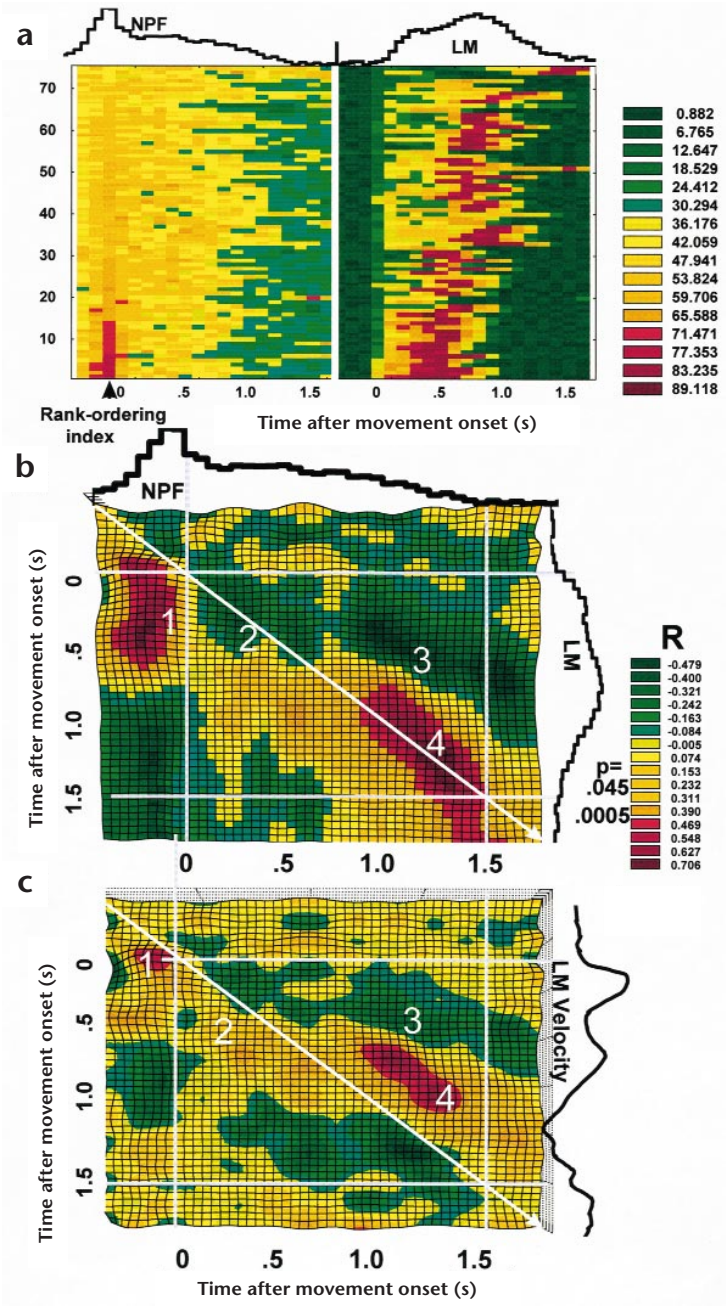

Fig. 5. Premovement NP activity predicts lever movement. **(a)** Rank-ordered peri-event rasters show NP-function activity (NPF; as in **Fig. 4**), left, and lever movement (LM), right, over the same 74 trials. Trials are rank ordered (from bottom) by peak amplitudes measured within the first 100 ms before lever movement. Traces at top show averaged NP function and lever movement. Colors show NP function amplitude or lever displacement as percentages between minima and maxima. **(b)** Time-shifted correlation matrix between the NP function and lever movement in Fig. 5a displayed as a spline-smoothed color-coded surface. Correlation coefficients (r) indicated at right. White diagonal line indicates correlations at zero time shift. In correlations to the left of this diagonal, the NP leads the movement (as for a 'motor' signal); right of the diagonal, the NP follows the movement (as for a 'sensory' response). Vertical and horizontal lines indicate lever-movement onset (at 0.0 s) and of lever release (1.5 s). Traces at top and right show averaged NP function and lever movement. **(c)** Correlogram similar to **(b)** correlating NP activity with lever velocity rather than displacement.

Therefore, this provided a test of whether the animal could adapt its operant behavior and/or its NP activity to the changed response criterion. These experiments were typically begun with a short period of lever-movement/robot-arm mode testing to confirm the normal correlation between the activity peak preceding lever movement and its initial trajectory (Fig. 6c, left). After switching to NP-function/robot-arm mode (Fig. 6c, right), animals typically continued to press the lever down to the original threshold position for obtaining the water for several trials, presumably reflecting the high correlation between lever movement and the preceding activity peak (Fig. 5b). During subsequent trials, however, this normally high correlation declined (from $r = 0.81$, $p = 0.004$ over the first 10 trials in Fig. 6c, right, to insignificant correlation for all subsequent sets of 10 trials). Even though the animal continued to make sporadic lever movements, usually following failures (for instance, trials 30 and 45 following 29 and 44), the animal was generally able to obtain water without moving the lever to the threshold routinely attained under the lever-movement/robot-arm mode. Indeed, 11 of these trials were rewarded without any lever movement, and in one trial, without even a forelimb-reaching movement, the animal simply resting its paw on the lever.

Similar results were obtained in all four animals able to work in the NP-function/robot-arm mode. By the second day of this conditioning, they all maintained a 60–100% success rate, even when the normally high correlation between lever movement and preceding activity peak ($r_{mean} = 0.65$) fell to insignificant levels ($r_{mean} = 0.15$). Despite these changes, analysis of the magnitude and timing of the first five principal components of the NP-function activity revealed no significant changes in the overall distribution of neuronal discharges. Thus, it is unlikely that the observed reduction in movement magnitude could be explained by a selective reduction of activity in a certain subclass of neurons in this population, in either the MI or the VL.

Discussion

This investigation demonstrated that information extracted from simultaneously recorded populations of single neurons in the brain can be used to proportionally drive an external motion device in real time. This was made possible by the recent availability of techniques for multisite, multineuron recording, and provides further evidence of the importance of activity across neuronal populations for information processing in the brain. The current results also corroborate previous suggestions[22–24] that neuronal populations surpass single neurons in the ability to smoothly encode brain information pertaining to a sensory image or a movement. Here this hypothesis was directly tested by requiring animals to use such neuronal population activity to control the robot arm to obtain water.

Another important finding was that representations of the spatiotemporal domain of neural information (using recurrent ANNs, for instance) predicted movement timing with greater accuracy than representions of the spatial domain alone. In particular, a short but highly synchronized period of neural activity (the pre-lever-movement peak) was a better predictor of lever

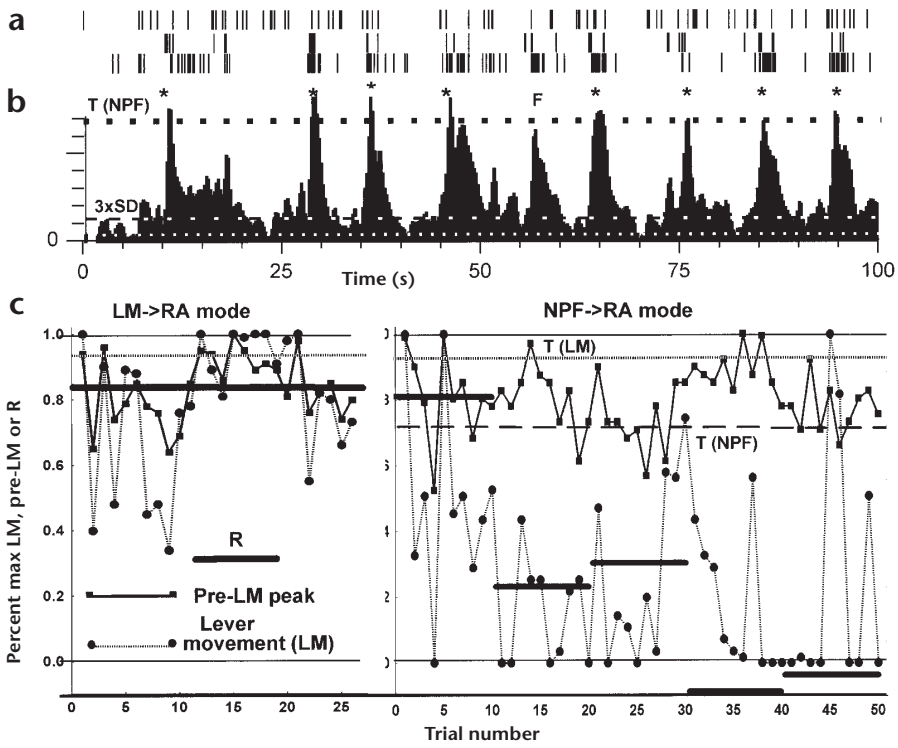

Fig. 6. Neurorobotic mode. **(a)** Spike trains from three neurons for 100 seconds after switching to NP-function/robot-arm (NPF/RA) mode. **(b)** NP function for the same period used to electronically drive a robot arm in realtime. Asterisks indicate pre-movement NP peaks in trials in which the robot arm was successfully moved to the water drop 'T (NPF)' using this real time NP signal. **(c)** NPF amplitude in the 100 ms before lever movement shows loss of correlation between the NPF and lever movement (LM) during continued training in NPF/RA mode. On day 2, the animal was first reconditioned in the LM/RA for 27 trials (left) followed by 50 trials in NPF/RA mode (right). Correlation coefficients (r) are indicated by thick horizontal lines over included trials. Significant correlation (p = 0.004) was found only in the first ten NPF/RA trials. 'T (LM)' indicates the threshold position and 'T(NPF)' indicates activity threshold for reward in LM/RA and NPF/RA modes, respectively. Animals failing to attain the T(LM) threshold in 500 ms of LM/RA often reached it with additional pressing.

movement than was neural activity recorded during the lever movement itself. This is consistent with our finding that distinct temporal patterns of multi-neuronal ensemble discharge in the monkey somatosensory cortex encode specific parameters of sensory stimulation[25].

We also demonstrated that the pre-lever-movement peak's normal ability to predict movement can be quickly modified by training in the neurorobotic mode. Thus, even though the pre-lever-movement peak normally shows 'movement coding' (as defined by the usual correlational approach), this does not guarantee an obligatory relationship with movement. Though this adaptability implies a level of abstraction normally ascribed to the premotor cortices, there is evidence that the MI shows similar functional adaptability[26]. Moreover, our findings are directly consistent with classic reports that MI cortical single units can be dissociated from movement by conditioning[27–31]. These results are also generally consistent with reports of remapping of motor output functions of the MI cortex after peripheral injury[32]. The current results also show that the NP function itself could rapidly replace overt movement as the operant behavior for this conditioning protocol. On the other hand, the context of voluntary movement was not extinguished, as our animals generally continued to reach to the lever, but not to press it. It seems, therefore, that this decorrelation of motor cortex neural activity from movement was facilitated by maintenance of the overall motor context. It is thus conceivable that the animals could have formed an internal representation of the intended movements and then aborted their expression.

The feasibility of using simultaneously recorded NPs to control external movement devices demonstrated by this study raises the possibility that paralyzed patients could use such recordings to control external devices or even their own muscles through functional electrical stimulation[33–35]. Considering the requirement for such patients to 'relearn' neural control of movement, it is notable that the current studies demonstrate modifiability of cortical NP codes. Finally, beyond this clinical application, the general strategy developed here of using brain-derived signals to control external devices may provide a unique new tool for investigating information processing within particular brain regions.

Methods

Implantation. Methods for surgery, multineuron recording and analysis have been published[3–6,11,16,17]. Briefly, six Long-Evans (hooded) rats were chronically implanted with arrays or bundles of microwire electrodes in the MI cortex and VL thalamus. Arrays consisted of two parallel rows of eight electrodes (2.0-mm long, rows separated by 0.5). Arrays were implanted rostrocaudally across layer V of the primary motor cortex (MI) forelimb area[36]; location was verified by microstimulation to produce forelimb movements at threshold (80–200 μA)[13], characterization of motor correlates (see Fig. 3) and histology. All MI cortical neurons described were 'forelimb-positive' by these criteria. Bundles were implanted in the VL thalamus within a ~1.0-mm radius. Two rats were also implanted with four bipolar EMG electrodes (twisted pairs of seven-stranded stainless steel, Medwire, Mt. Vernon, New York) in forelimb muscles, including the triceps and biceps long head and extensor and flexor carpi/digitorum muscles.

Signal processing. Approximately one week after surgery, animals were placed in the behavior chamber, and their head-mounted chronic implants were connected via a wire harness to a 64-channel Many-Neuron-Acquisition-Processor (MNAP; Plexon, Dallas, Texas). Amplified and filtered waveforms from one to two single neurons (at least 5× noise) per channel were continuously discriminated using on-screen manipulation of multiple time–voltage windows. Times of single neuron (and also multi-motor-unit) action potentials were stored on a Motorola VME 162 computer, synchronized with analog recordings of robot-arm position and videotape recordings of the animals' motor behavior. Discriminated waveforms (40 kHz resolution; Fig. 1) could be uploaded into a PC computer for off-line graphical display and analysis. Timing pulses for each of 32 discriminated action potentials were also routed via separate channels into a real-time 32-channel, spike-integrator board to generate a single analog signal to control robot arm position.

Both single neuron and neuronal population function signals were

analyzed using Stranger (Biographics, Winston-Salem, North Carolina) and NEX (Plexon, Dallas, Texas) to generate stripcharts, peri-event histograms (PEHs), rasters and correlograms. Significant events for such analysis were obtained from the lever output, field-by-field analysis of videotapes (17-ms resolution, system from Lafayette Instruments, Lafayette, Indiana) and EMG recordings. PEHs were used to initially characterize single-neuron movement correlates. To visualize the statistical dispersion in such PEHs, bins were standardized by subtracting the mean and dividing by the standard deviation (Fig. 2), allowing one confidence interval to be calculated for all histogram bins. The Kolmogorov-Smirnov one-sample test was also used as a non-parametric, robust and relatively assumption-free statistical method for evaluating PEH results. Significance among multiple neurons was assessed using a multivariate analysis of variance (MANOVA), typically with a repeated measures, single-factor design across non-overlapping experimental groups. Discriminant function analysis (DFA)[6–7] was performed by randomly dividing the data from the neuronal population into a learning set and a test set (Statistica, StatSoft, Tulsa, Oklahoma).

Two techniques were used to transform the timing pulses for the discriminated action potentials of simultaneously recorded neurons into neuronal population functions[21]. Principal components analysis (PCA) was used to generate linear neuronal population functions based on recurring patterns of covariance among the neuronal activity as previously described[5,21,22]. PCA provides weighting of each neuron's contribution to the population average according to its patterns of correlation with other neurons, thereby concentrating the salient 'signal' embedded within the neural activity into a small number of orthogonal principal components and effectively separating them from the stochastic activity of individual neurons. PCA involved eigenvalue rotation of the correlation matrix between firing rates in equivalent time bins of recorded neurons. This produced a set of principal components (eigenvectors) that explained successively smaller amounts of the total variance. Components could be reconstructed as a weighted population average of the recorded neurons using the rotational coefficients as weights.

Spatio-temporal transformations using recurrent artificial neural networks (ANNs). The ANNs were built using the 'Neurosolutions' package (Neural Dimensions, Gainesville, Florida). Dynamic back-propagation learning (using the learning data set) was used to adjust the weightings within this network to optimally transform the NP input (from the test data set) into an output function that closely matched the lever-movement predictor function (Fig. 4d). Testing was carried out only after the mean-squared error of the prediction (loss function) asymptotically reached a minimum level.

Acknowledgements

This work was supported by NIH contract NS62352, ONR grant N00014-98-1-0679 and NIH grant NS26722 to J.K.C.

RECEIVED 8 FEBRUARY; ACCEPTED 25 MAY 1999

1. Georgopoulos, A. P., Kettner, R. E. & Schwartz, A. B. Neuronal population coding of movement direction. *Science* 233, 1416–1419 (1986).
2. Erickson, R. Stimulus coding in topographic and nontopographic afferent modalities: on the significance of the activity of individual sensory neurons. *Psychol. Rev.* 75, 447–465 (1968).
3. Nicolelis, M. A., Ghazanfar, A. A., Faggin, B. M. Votaw S. & Oliveira L. M. Reconstructing the engram: simultaneous, multisite, many single neuron recordings. *Neuron* 18, 529–537 (1997).
4. Nicolelis, M. A., Lin, C.-S., Woodward, D. J. & Chapin, J. K. Distributed processing of somatic information by networks of thalamic cells induces time-dependent shifts of their receptive fields. *Proc. Natl. Acad. Sci. USA* 90, 2212–2216 (1993).
5. Nicolelis, M. A., Baccala, L. A., Lin, C.-S. & Chapin, J. K. Synchronous neuronal ensemble activity at multiple levels of the rat somatosensory system anticipates onset and frequency of tactile exploratory movements. *Science* 268, 1353–1358 (1995).
6. Nicolelis, M. A., Lin, C.-S. & Chapin, J. K. Neonatal whisker removal reduces the discrimination of tactile stimuli by thalamic ensembles in adult rats. *J. Neurophysiol.* 78, 1691–1706 (1997).
7. Deadwyler, S. A. & Hampson, R. E. The significance of neural ensemble codes during behavior cognition. *Annu. Rev. Neurosci.* 20, 217–244 (1997).
8. Chapin, J. K. & Woodward, D. J. Distribution of somatic sensory and active-movement neuronal discharge properties in the MI–SI cortical border area in the rat. *Exp. Neurol.* 91, 502–523 (1986).
9. Chapin, J. K. & Woodward, D. J. Somatic sensory transmission to the cortex during movement: I. Gating of single cell responses to touch. *Exp. Neurol.* 78, 654–669 (1982).
10. Chapin, J. K. & Woodward, D. J. Somatic sensory transmission to the cortex during movement: II. Phasic modulation over the locomotor step cycle. *Exp. Neurol.* 78, 670–684 (1982).
11. Shin, H.-C. & Chapin, J. K. Movement-induced modulation of afferent transmission to single neurons in the ventroposterior thalamus and somatosensory cortex in rat. *Exp. Brain Res.* 81, 515–522 (1990).
12. Chapin, J. K. in *Neural and Behavioral Approaches to Higher Brain Function* (eds. Wise, S. P. & Evarts, E. V.)201–216 (Wiley, New York, 1987).
13. Evarts, E. V. Relation of pyramidal tract activity to force exerted during voluntary movement. *J. Neurophysiol.* 31, 14–27 (1968).
14. Ghez, C., Vicario, D., Martin, J. H. & Yumiya, H. Role of the motor cortex in the initiation of voluntary motor responses in the cat. *Electroencephalogr. Clin. Neurophysiol. Suppl.* 36, 409–414 (1982).
15. Donoghue J. P. Contrasting properties of neurons in two parts of the primary motor cortex of the awake rat. *Brain Res.* 333, 173–177 (1985).
16. Chapin, J. K. in *Neuronal Population Recording* (ed. Nicolelis, M. A.)193–228 (CRC Press, Boca Raton 1998).
17. Chapin, J. K. & Nicolelis, M. A. Neural network mechanisms of oscillatory brain states: characterization using simultaneous multi-single neuron recordings. *Electroencephalogr. Clin. Neurophysiol. Suppl.* 45, 113–122 (1996).
18. Evarts, E. V. Pyramidal tract activity associated with a conditioned hand movement in the monkey. *J. Neurophysiol.* 29, 1011–1027 (1966).
19. Schmidt, E. M., Jost, R. G. & Davis, K. K. Reexamination of the force relationship of cortical cell discharge patterns with conditioned wrist movements. *Brain Res.* 83, 213–223 (1975).
20. Scott, S. H. & Kalaska, J. F. Changes in motor cortex activity during reaching movements with similar hand paths but different arm postures. *J. Neurophysiol.* 73, 2563–2567 (1995).
21. Moore, G. P., Perkel, D. H. & Segundo, J. P. Statistical analysis and functional interpretation of neuronal spike data. *Annu. Rev. Physiol.* 28, 493–522 (1966).
22. Humphrey, D. R., Schmidt, E. M. & Thompson, W. D. Predicting measures of motor performance from multiple cortical spike trains. *Science* 170, 758–762 (1970).
23. Dormont, J. F., Schmied, A. & Condé, H. Motor command in the ventrolateral thalamic nucleus: neuronal variability can be overcome by ensemble average. *Exp. Brain Res.* 48, 315–322 (1982).
24. Lukashin, A.V., Amirikian, B. R. & Georgopoulos, A. P. A simulated actuator driven by motor cortical signals. *Neuroreport* 7, 2597–2601 (1996).
25. Nicolelis, A. L. *et al.* Simultaneous representation of tactile information by distinct primate cortical areas rely on different encoding strategies. *Nat. Neurosci.* 1, 621–630 (1998).
26. Wise, S. P., Moody, S. L., Blomstrom, K. J. & Mitz, A. R. Changes in motor cortical activity during visuomotor adaptation. *Exp. Brain Res.* 121, 285–299 (1998).
27. Fetz, E. E. Operant conditioning of cortical unit activity. *Science* 28, 955–958 (1969).
28. Fetz, E. E. & Finocchio, D. V. Operant conditioning of specific patterns of neural and muscular activity. *Science* 174, 431–435 (1971).
29. Fetz, E. E. & Finocchio, D. V. Operant conditioning of isolated activity in specific muscles and precentral cells. *Brain Res.* 40, 19–23 (1972).
30. Fetz, E. E. & Baker, M. A. Operantly conditioned patterns on precentral unit activity and correlated responses in adjacent cells and contralateral muscles. *J. Neurophysiol.* 36, 179–204 (1973).
31. Fetz, E. E. & Finocchio, D. V. Correlations between activity of motor cortex cells and arm muscles during operantly conditioned response patterns. *Exp. Brain Res.* 23, 217–240 (1975).
32. Sanes, J. N., Suner, S., Lando, J. F. & Donoghue, J. P. Rapid reorganization of adult rat motor cortex somatic representation patterns after motor nerve injury. *Proc. Natl. Acad. Sci.* 85, 2003–2007 (1988).
33. Schmidt, E. M. Single neuron recording from motor cortex as a possible source of signals for control of external devices. *Ann. Biomed. Eng.* 8, 339–349 (1980).
34. Kennedy, P. R. & Bakay, R. A. Restoration of neural output from a paralyzed patient by a direct brain connection. *Neuroreport* 9, 1707–1711 (1998).
35. Bhadra, N. & Peckham P. H. Peripheral nerve stimulation for restoration of motor function. *J. Clin. Neurophysiol.* 14, 378–393 (1997).
36. Donoghue, J. P. & Wise, S. P. The motor cortex of the rat: cytoarchitecture and microstimulation mapping. *J. Comp. Neurol.* 212, 76–88 (1982).